The Aggregation of Trichosanthin in Aqueous Solution

CHI WU,[1]* PEIQIANG WU,[2] and XING-QI MA[3]

[1]Department of Chemistry, The Chinese University of Hong Kong, Shatin, N.T., Hong Kong; [2]Department of Chemistry, Peking University, Beijing, China; [3]Institute of Biophysics, Academia Sinica, Beijing, China

SYNOPSIS

As a kind of cytotoxin extracted from the root tuber of *Trichosanthes kirilowii Maxim* (Cucurbitaceae), trichosanthin can selectively bind to and kill the placental trophoblastic cells, which leads to a number of biomedical applications including the inhibition of trophoblastic tumors. However, the stability of trichosanthin in living organism is still one of the problems hindering the effectiveness of its applications. In this study, laser light scattering has been used successfully to investigate the stability of trichosanthin in both deionized water and KSCN aqueous solution in terms of the hydrodynamic size distribution of the trichosanthin aggregates as a function of both time and the salt concentration. It is found that the size distribution is always a bimodal one. One peak corresponds to a single trichosanthin chain; the other corresponds to the trichosanthin aggregates, which have an average hydrodynamic radius of $\sim$ 49 nm and are composed of $\sim$ 127 trichosanthin molecules when C_{KSCN} is higher than 0.5 mol/L. This implies that there exists an equilibrium between the single trichosanthin chain and its aggregates [i.e., $nT \rightleftarrows (T)_n$]. Our results also suggest that the aggregates are made of the loosely packed trichosanthin molecules and behave as flexible polymer chains in Θ solvent. © 1996 John Wiley & Sons, Inc.

Keywords: trichosanthin • aggregation • laser light scattering

INTRODUCTION

Trichosanthin extracted from the root tuber of *Trichosanthes kirilowii Maxim* (Cucurbitaceae) is an effective plant protein of a popular Chinese herb medicine and a kind of cytotoxin. Cell biological studies have shown that it can bind selectively to and kill the placental trophoblastic cell.[1] Originally, it has been widely used in the folk remedy for treating many diseases, such as the dead fetus in uterus, hydatidiform mole, and ectopic pregnancy, to name just a few. Recently, it was reported that it can be used to inhibit trophoblastic tumors and may also be useful in treatment of the AIDS disease,[2] which have certainly attracted more attention to this kind of cytotoxin and its applications.

Trichosanthin is a single-chain protein ($pI \sim 9.4$ and $M \sim 2.7 \times 10^4$ g/mol) containing 247 amino acid residues, which is different from normal cytotoxins composed of two types of subunits.[3] The three-dimensional structure of trichosanthin was derived from the monoclinic C2 and orthorhombic P212121 crystal structure determination[4,5] and the complete sequence has been determined,[6] which indicates that trichosanthin is homologous to one of the two subunits of toxic ricin.[7] As a drug, the crystalline form of trichosanthin is used and administered in one injection of a 1–2 mg dose. However, the successful crystallization of trichosanthin is impeded by microheterogeneity that might arise from the formation of various states of aggregation in a relatively concentrated solution during the crystallization process. In aqueous solution, both the type and amount of added salts will have an additional influence on the stability or the aggregation process. Therefore, a better understanding of the stability of trichosanthin in aqueous solution with and without adding low molecular weight electrolytes will be important to its crystallization process.

As a nonintrusive and sensitive analytical method, laser light scattering (LLS), especially dynamic LLS, has been widely used in both macromolecular and colloid sciences to characterize and study polymers and particles.[8–10] In this work, it is

* To whom correspondence should be addressed.

Journal of Polymer Science: Part B: Polymer Physics, Vol. 34, 221–227 (1996)
 CCC 0887-6266/96/020221-07

our intention to use LLS to study the stability of trichosanthin by measuring the hydrodynamic radius (R_h) distribution of the aggregates as a function of both time and salt concentration; to determine the average number of trichosanthin molecules inside each aggregate; and to reveal the aggregation process and the structure of the aggregates.

Basic Theories

Static Light Scattering

The angular dependence of the excess absolute time-averaged scattered intensity, known as the excess Rayleigh ratio [$R_{vv}(\theta)$], was measured. For a dilute solution at concentration C (g/ml) and the scattering angle θ, $R_{vv}(\theta)$ can be approximately expressed as[11]

$$\frac{KC}{R_{vv}(\theta)} \cong \frac{1}{M_w}\left(1 + \frac{1}{3}\langle R_g^2\rangle q^2\right) + 2A_2C \qquad (1)$$

where $K = 4\pi^2 n^2\left(\frac{dn}{dC}\right)^2 \Big/ (N_A\lambda_0^4)$ and $q = \frac{4\pi n}{\lambda_0}\sin\left(\frac{\theta}{2}\right)$

with N_A, dn/dC, n, and λ_0 being Avogadro's number, the specific refractive index increment, the solvent refractive index, and the wavelength of light in vacuo, respectively. M_w is the weight average molar mass of dissolved polymers or suspended aggregates, A_2 is the second-order virial coefficient and $\langle R_g^2\rangle^{1/2}$, or simply as R_g, is the root-mean-square average radius of gyration of the polymer. By measuring $R_{vv}(\theta)$ at a set of C and θ, we were able to obtain M_w, R_g, and A_2 from a Zimm plot, which put the dependence of $KC/R_{vv}(\theta)$ on both C and θ in a single grid.[11]

Dynamic Light Scattering

An intensity–intensity time correlation function $G^{(2)}(n\Delta\tau, \theta)$ in the self-beating mode is normally measured, which has the following form[12,13]

$$G^{(2)}(t, \theta) = \langle I(t, \theta)I(0, \theta)\rangle = A[1 + \beta|g^{(1)}(t, \theta)|^2] \qquad (2)$$

where A is a measured baseline, β is a parameter depending on the coherence of the detection, t is the delay time, and $g^{(1)}(t, \theta)$ is the normalized first-order electric field $E(t)$ time correlation function. $g^{(1)}(t, \theta)$ is related to the line-width distribution $G(\Gamma)$ by

$$g^{(1)}(t, \theta) = \langle E(t, \theta)E^*(0, \theta)\rangle = \int_0^\infty G(\Gamma)e^{-\Gamma t}\,d\Gamma. \qquad (3)$$

$G(\Gamma)$ can be calculated from $g^{(1)}(t, \theta)$, or $G^{(2)}(t, \theta)$, by Laplace inversion or by a cumulant expansion of eq. (3), that is,

$$\ln(g^{(1)}(t)) = -\bar{\Gamma}q^2t + \sum_{n=2}^{\infty}(-1)^n\frac{\mu_n(\Gamma)(q^2t)^n}{n!} + \cdots \qquad (4)$$

where $\bar{\Gamma} = \int_0^\infty G(\Gamma)\Gamma\,d\Gamma$, $\mu_n(\Gamma) = \int_0^\infty G(\Gamma)(\Gamma - \bar{\Gamma})^n\,d\Gamma$, and $\mu_2(\Gamma)/\bar{\Gamma}^2$ is the variance that characterizes the distribution width. In most cases, n is not larger than 3. Γ or $\bar{\Gamma}$ normally depends on both C and θ as[13]

$$\frac{\Gamma}{q^2} = D(1 + k_dC)(1 + f\langle R_g^2\rangle_z q^2) \qquad (5)$$

where k_d is the diffusion second virial coefficient and f is a dimensionless number. At $C \to 0$ and $\theta \to 0$, $\Gamma/q^2 \to D$. Therefore, with a pair of known k_d and f, we can transfer $G(\Gamma)$ obtained in a finite concentration and at a certain scattering angle into a translational diffusion coefficient distribution $G(D)$ that can be further reduced into a hydrodynamic radius (R_h) distribution by using the Stokes-Einstein equation,

$$R_h = \left(\frac{k_BT}{6\pi\eta}\right)D^{-1} \qquad (6)$$

where k_B, T, and η are the Boltzmann constant, the absolute temperature, and the solvent viscosity, respectively.

EXPERIMENTAL METHODS

Sample Preparation

Trichosanthin can be prepared by the fractional acetone precipitation of the juice from the fresh tuber of *Trichosanthes*. The purification of the crude acetone precipitate can be achieved by either the crystallization in barbiturate buffer (pH 8.6)[14] or applying it to a CM-Sephadex G-50 column twice.[15] The purity of crystalline trichosanthin was better than 99%.[16] Both the trichosanthin and analytical grade potassium thiocyanate (KSCN) were used without further recrystallization in this study. First, the KSCN aqueous solution was prepared by dissolving KSCN in double-distilled deionized water and the KSCN concentration was in the range of 0–1.0 mol/L; then 4-mg trichosanthin (except in

static LLS where different amounts of trichosanthin were used) was added in a 10-mL KSCN aqueous solution to form a trichosanthin aqueous solution with $C = 4 \times 10^{-4}$ g/mL; and finally, the trichosanthin aqueous solution was clarified by a 0.22 μm Millipore filter to remove dust. The pH value of the final solution was 7.2. The time from adding trichosanthin in the KSCN aqueous solution to the start of the LLS measurement was about 15 min, which was the minimum time required to prepare the final/clean trichosanthin solution and to establish the good temperature equilibrium at 15°C. In static LLS, the exact concentrations of trichosanthin in the solution were determined in the following two steps: ultracentrifugation and then freeze dry. The estimated 8% water inside the dried protein has been taken into account in the calculation of final protein concentration.

Laser Light Scattering

A commercial LLS spectrometer (ALV-5000, Langen in Hessen, Germany) was used with an argon-ion laser (Coherent INNOVA 90, operated at 488 nm and 400 mW) as light source. The primary beam is vertically polarized. In our present setup, the value of β is about 0.85, which is rather high for an LLS spectrometer capable of doing both static and dynamic LLS measurements, so that we are able to carry out dynamic LLS of very dilute solutions. The instrument has supplied both the cumulant analysis and Laplace inversion (CONTIN) programs. The detail of LLS theory, instrumentation, and data analysis can be found elsewhere.[12,13] All LLS measurements were carried out at 15.0 ± 0.1°C.

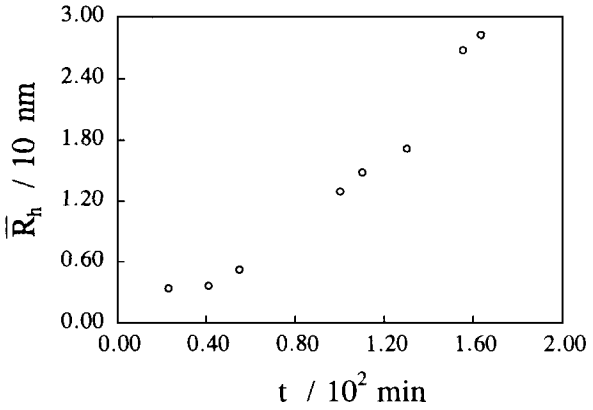

Figure 1. Hydrodynamic radius $\bar{R}_h$ of trichosanthin in deionized water versus time, where $\bar{R}_h$ was calculated from $\bar{D}$ and $\bar{D}$ was from the second-order cumulant analysis of the measured time correlation function.

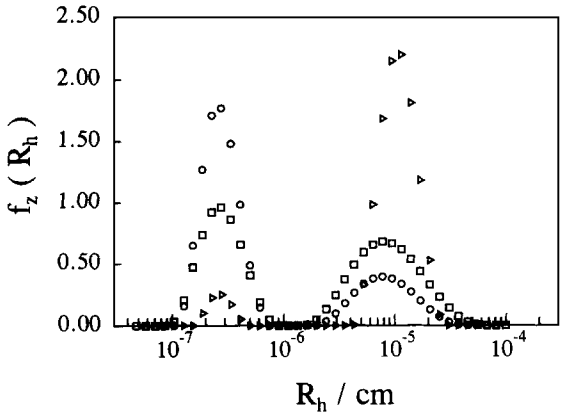

Figure 2. Intensity-weighted hydrodynamic radius distribution $f_z(R_h)$ of trichosanthin in deionized water after different dissolving time: (○) t = 23 min; (□) t = 55 min; and (△) t = 163 min.

RESULTS AND DISCUSSION

Figure 1 shows the overall average hydrodynamic radius $\bar{R}_h$ of trichosanthin in deionized water versus time, where $\bar{R}_h$ was obtained by replacing D with $\bar{D}$ from the second-order cumulant analysis of the measured time correlation function. Figure 1 apparently indicates that $\bar{R}_h$ increases rapidly with time (i.e., the aggregate becomes larger and larger). However, a further Laplace analysis of the measured time correlation function [i.e., $G(\Gamma)$] shows a different picture.

Figure 2 shows three intensity-weighted hydrodynamic radius distribution $f_z(R_h)$ of trichosanthin in deionized water at different times, where $f_z(R_h)$ were obtained from $G(\Gamma)$ on the basis of $\Gamma = q^2D$ and eq. (6). The subscript "z" implies that the distribution is an intensity one, which means that $f_z(R_h) \propto f_n(R_h)M^2$ where $f_n(R_h)$ is the number distribution. It shows that $f_z(R_h)$ is always a bimodal distribution. The position of the peak located at ~ 2.8 nm is basically independent on time and this peak corresponds to individual trichosanthin molecules because the molecular dimension of trichosanthin is known to be $4.9 \times 3.8 \times 3.7$ nm^3; the other peak with the center located in the range of ~ 80–100 nm should represent the aggregates of trichosanthin molecules.

Figure 3 shows the peak area ratio A/A_T versus time for each of the two peaks in Figure 2, where A_T is the total area under the two peaks. It clearly shows that the amount of individual trichosanthin molecules diminishes as time increases whereas the number of the trichosanthin aggregates increases at the same time. A combination of Figure 2 and 3

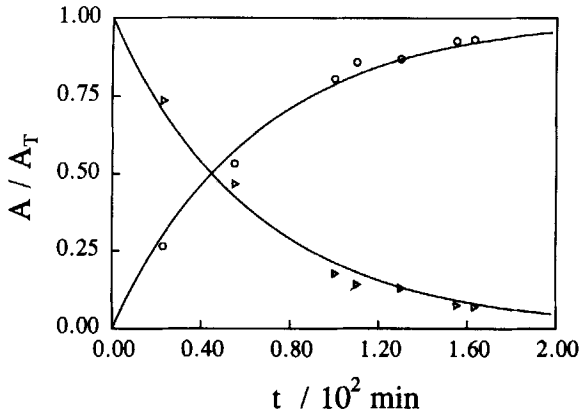

Figure 3. Peak area ratio A/A_T versus time for each of the two peaks in Figure 2, where A_T is the total area under the two peaks. (○) The aggregate's peak and (△) the individual trichosanthin molecule's peak.

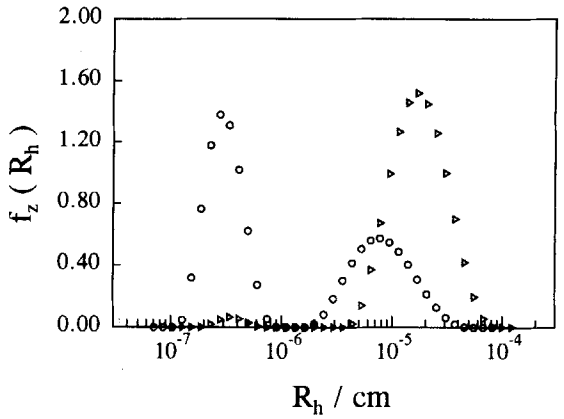

Figure 4. Intensity-weighted hydrodynamic radius distributions $f_z(R_h)$ of trichosanthin in 0.05M KSCN aqueous solution after different dissolving times: (○) short time and (△) long time.

indicates that trichosanthin is not stable in deionized water and undergoes an aggregation process of "n(trichosanthin) → (trichosanthin)$_n$" where the number "n" changes with time, but not too much, because the peak position basically remains within a small size range. This process can be fitted apparently by a first-order reaction kinetics (the lines in Fig. 3),

$$A/A_T = 1 - e^{-kt} \quad \text{(for the aggregates)}$$

or

$$A/A_T = e^{-kt} \quad \text{(for trichosanthin)} \qquad (7)$$

with $k = (1.55 \pm 0.02) \times 10^{-2}\ \text{min}^{-1}$, which implies that the aggregation was formed by one trichosanthin at a time. It is known that, besides the hydrophobic interaction between the protein backbone chain, there are two kinds of interactions in the protein aqueous solution. One is caused by the static charges on the protein chain and the other by the hydrogen bonding. Without adding KSCN, the static charges will lead to the intermolecular repulsions that should prevent the aggregation. Therefore, the observed aggregation process is fast, which might imply that the hydrogen bonding plays a dominate role in the aggregation of trichosanthin. On the basis of the study of trichosanthin in deionized water, we realized that the overall mean hydrodynamic radius could seriously mislead to a complete wrong conclusion. Therefore, we have to use the hydrodynamic radius distribution throughout this study.

Figure 4 shows two intensity-weighted hydrodynamic radius distributions $f_z(R_h)$ of trichosanthin in 0.05M KSCN aqueous solution. One was obtained just after dissolving trichosanthin in the solution and the other a long time after dissolving trichosanthin in the solution. Figure 4 shows that the hydrodynamic radius of the aggregates gradually increases from ~ 70 to ~ 180 nm and at the same time the amount of individual trichosanthin molecules decreases; that is, the aggregation took place in the presence of a small amount (0.05M) of KSCN in the solution as an electrolyte. Naturally, we like to ask what will happen if more KSCN is added into the trichosanthin aqueous solution.

Figure 5 shows two intensity-weighted hydrodynamic radius distributions $f_z(R_h)$ of trichosanthin in 0.5M KSCN aqueous solution at different times after dissolving trichosanthin in the solution. The two distributions are essentially the same, which clearly shows that in the presence of 0.5M KSCN

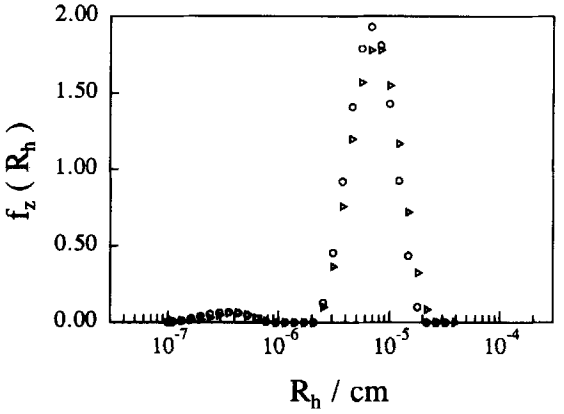

Figure 5. Intensity-weighted hydrodynamic radius distributions $f_z(R_h)$ of trichosanthin in 0.5M KSCN aqueous solution after different dissolving time: (○) short time and (△) long time.

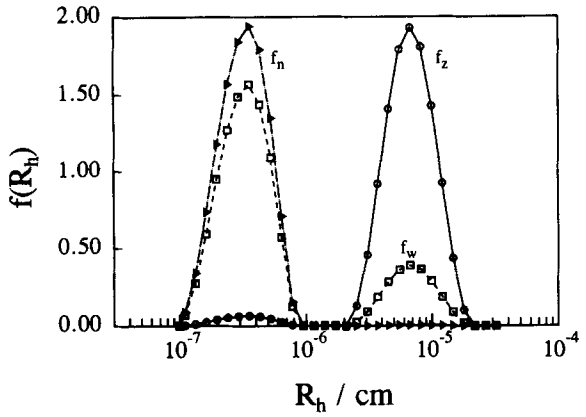

Figure 6. Intensity-, weight-, and number-weighted hydrodynamic radius distributions of trichosanthin in 0.5M KSCN aqueous solution, where f_z is an intensity distribution; f_w is a weight distribution, and f_n is a number distribution.

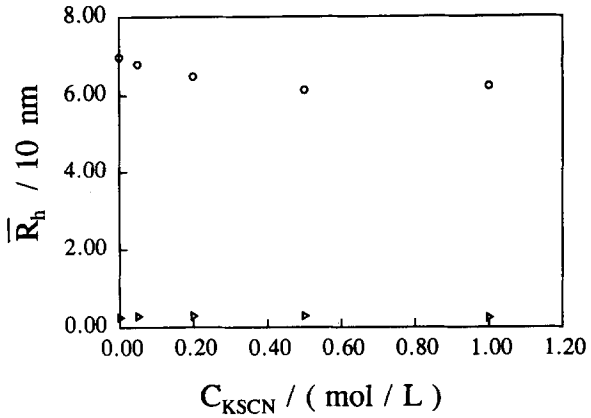

Figure 7. Average hydrodynamic radius $\bar{R}_h$ versus C_{KSCN} (the concentration of KSCN) for the aggregate peak (○) and the individual trichosanthin molecule peak (△), where $\bar{R}_h$ was measured just after trichosanthin was dissolved in the solution for a short time period of 15 min.

the aggregation is almost completed instantly and reaches to an equilibrium between individual trichosanthin molecules and their aggregates. It should be noted that the larger peak area of the trichosanthin aggregate in $f_z(R_h)$ actually represents only a small amount of the aggregates in terms of weight because $f_z(R_h)$ is an intensity distribution.

Figure 6 shows the intensity-, weight-, and number-weighted hydrodynamic radius distributions of trichosanthin in 0.5M KSCN aqueous solution, where f_z is an intensity distribution, f_w is a weight distribution, and f_n is a number distribution. It shows that the number of the trichosanthin aggregates is really small even though their contribution to the scattered intensity is high. This is understandable because on the basis of eq. (1) the scattered intensity is proportional to M_w or wM or nM^2. The mass difference between individual trichosanthin molecule and the aggregate is more than 100 times; that is, the light scattered by a single aggregate could be as high as that by more than $\sim 10^4$ individual trichosanthin molecules. Therefore, LLS, especially dynamic LLS, is a very sensitive method to detect the presence of larger aggregates in a given system. The estimated amount of the aggregates in terms of weight in Figure 6 is about 20%.

Figure 7 shows the average hydrodynamic radius $\bar{R}_h$ versus the KSCN concentration C_{KSCN} for the aggregate's peak and the individual trichosanthin molecule's peak, where $\bar{R}_h$ was measured just after trichosanthin was dissolved in the solution for a short time period of 15 min, which is the shortest and experimentally achievable time. It is understandable that there is no change in $\bar{R}_h$ for the individual trichosanthin molecule's peak because the size of individual molecules is not greatly influenced by the amount of the added salt. On the other hand, when $C_{KSCN} \geq 0.5M$, the size of the aggregates decreases as C_{KSCN} increases and approaches a constant value of $\sim$ 63 nm, where we should note that the concentration of trichosanthin is finite. In the presence of KSCN, static charges on trichosanthin are partially shielded, so that trichosanthin molecules are able to approach each other more closely, which leads to a smaller aggregate.

Figure 8 shows the peak area ratio A/A_T versus C_{KSCN} for both the individual trichosanthin mole-

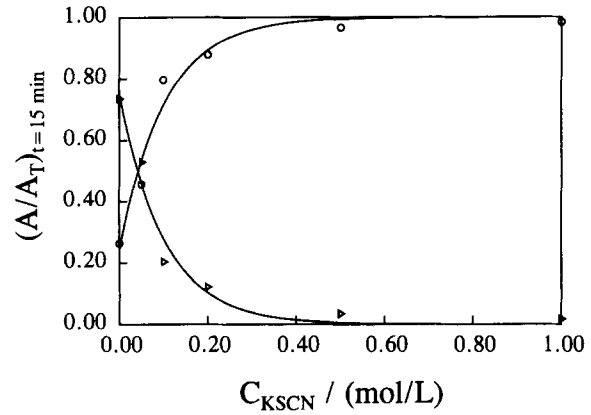

Figure 8. Peak area ratio A/A_T versus C_{KSCN} for both the individual trichosanthin molecule peak (△) and the aggregate peak, where A_T is the total area under these two peaks and the subscript "t = 15 min" means that all values of A/A_T were obtained after dissolving trichosanthin in the solution for $\sim$ 15 min (i.e., the measurable initial stage).

Table I. Static and Dynamic LLS Results of Trichosanthin in 1 M KSCN Aqueous Solution at 15°C

$10^{-6}M_w$ (g/mol)	10^4A_2 (mol·mL/g^2)	R_g (nm)	$10^8\bar{D}$ (cm^2/s)	$\bar{R}_h$ (nm)	$10^{-3}k_d$ (mL/g)	f	$R_g/\bar{R}_h$
3.23	−6.7	70	3.8	49	−2.5	~ 0	1.43

The relative errors: M_w, ±5%; A_2 and k_d, ±10%; R_g, ±5%; $\bar{D}$ and $\bar{R}_h$, ±2%; and $R_g/\bar{R}_h$, ±7%.

cule's peak and the aggregate's peak, where A_T is the total area under these two peaks and the subscript "t = 15 min" means that all values of A/A_T in Figure 8 were obtained after dissolving trichosanthin in the solution for ~ 15 min (i.e., the measurable initial stage). The dependence of A/A_T on C_{KSCN} can be empirically formulated as

$$A/A_T = 1 - k_1 e^{-k_2 C_{KSCN}} \quad \text{(for the aggregates)}$$

or (7)

$$A/A_T = k_1 e^{-k_2 C_{KSCN}} \quad \text{(for trichosanthin)}$$

with $k_1 = 0.756 \pm 0.002$ and $k_2 = 9.90 \pm 0.08$ (L/mol). Figure 8 shows that the more KSCN is added, the faster the aggregation process of "n (trichosanthin) → (trichosanthin)$_n$" will be. When $C_{KSCN} \geq 0.5M$, the aggregation process is nearly finished and reaches to an equilibrium between the individual trichosanthin molecules and the aggregates before we are able to start the first initial LLS measurement.

It is at the condition of $C_{KSCN} = 1.0M$ and the equilibrium state that the trichosanthin aggregates were characterized by both static and dynamic LLS on a set of trichosanthin solutions, where the trichosanthin concentration ranges from 2.77×10^{-5} to 1.11×10^{-4} g/mol. The LLS data were analyzed on the basis of eqs. (1) and (5) and the final results are summarized in Table I. Because the molecular mass of trichosanthin is 2.7×10^4 g/mol, we are able to deduce the aggregation number (N_a), that is, the average number of trichosanthin molecules in one aggregate, from the mass of the aggregates, namely $N_a = 3.2 \times 10^6/2.7 \times 10^4 \cong 120$. It is known that for a uniform hard sphere, $R_g/R_h = 0.774$; for a highly branched polymer cluster, $R_g/R_h \sim 1.0$–1.1;[9] and for a linear and flexible polymer chain in good solvent, $R_g/R_h \sim 1.5$–1.8.[17-19] Our result ($R_g/R_h = 1.43$) clearly indicates that the trichosanthin aggregates are far from that of a densely packed uniform sphere, but instead consist of many loosely connected trichosanthin molecules and behave as random coil in Θ condition because the experimental value of R_g/R_h for a flexible chain in Θ condition is ~ 1.4.[20] This is only one of the possible conformations. In addition, on the basis of the scaling relationship $M \propto R_h^{\alpha}$, we are able to estimate that $\alpha = 1.67$ from the values of M and R_h of individual trichosanthin molecules and the aggregates. This value of α is typical for a polymer coil.[21] A better value of α can be determined by small-angle x-ray scattering. At the present stage, it is still not clear why the aggregation number approaches a constant value of ~ 120 and how trichosanthin molecules are aggregated together to form a coil-like (or say, loose and open) structure, which are subjects for further study.

CONCLUSION

This study has shown that trichosanthin is not stable and always aggregates in aqueous solution with or without KSCN as low molecular weight electrolyte. The amount of aggregates by weight is ~ 20%. With KSCN, the aggregation process is much faster than that in pure water. The aggregation process follows the first-order kinetics. When the concentration of KSCN is higher than $0.5M$, an equilibrium between individual trichosanthin molecules and the aggregates will be instantly reached. At equilibrium, the radius of the trichosanthin aggregates is ~ 49 nm. A combination of static and dynamic laser light scattering results reveals that on average each aggregate is composed of ~ 120 trichosanthin molecules and the aggregates are made of loosely connected trichosanthin molecules. Each aggregate in aqueous solution might have a similar conformation as polymer coil in solution.

The financial support of this work by the RGC (the Research Grants Council of Hong Kong Government) Earmarked Grant 1994/95 (CUHK 299/94P, 221600260) is gratefully acknowledged.

REFERENCES AND NOTES

1. The Second Laboratory, Shanghai Experimental Biology Institute, *Acta Zool. Sin.*, **22,** 126 (1974).
2. M. S. Mcgrath, *Proc. Natl. Acad. Sci. USA,* **86,** 2844 (1989).
3. S. Olsnes and A. Pihl, *Molecular Action of Toxins and Viruses,* Elsevier Biomedical Press, Amsterdam, 1982, pp. 51–105.
4. K. Z. Pan, X. Q. Ma, and C. Z. Ni, *Sci. Sin.*, **30(B),** 386 (1987).
5. X. Q. Ma, L. Jin, and D. C. Wang, XVI Congress and General Assembly International Union Crystallography, Beijing, China, 21–29 August, p. 121, 1993.
6. E. T. Colling, J. D. Robertus, and M. Lopresti, *J. Biol. Chem.*, **265,** 8665 (1990).
7. X. Zhang and J. Wang, *Nature,* **321,** 477 (1986).
8. C. Wu, *Macromolecules,* **26,** 3821 (1993).
9. C. Wu, J. Zuo, and B. Chu, *Macromolecules,* **22,** 633 (1989).
10. C. Wu, *Macromolecules,* **27,** 298 (1994).
11. B. H. Zimm, *J. Chem. Phys.*, **16,** 1099 (1948).
12. B. Chu, *Laser Light Scattering* (2nd ed.), Academic Press, New York, 1991.
13. R. Pecora, *Dynamic Light Scattering,* Plenum Press, New York, 1976.
14. S. W. Jin and X. X. Sun, *Acta Chim. Sin.*, **39,** 917 (1981).
15. Y. H. Wang and J. F. Ling, *Acta Zool. Sin.*, **23,** 176 (1976).
16. M. X. Li, H. W. Yeung, L. P. Pan, and Sunney I. Chan, *Nucleic Acids Res.*, **19,** 6309 (1991).
17. K. Huber, S. Bantle, P. Lutz, and W. Burchard, *Macromolecules,* **18,** 1461 (1985).
18. A. Z. Akcasu and C. C. Han, *Macromolecules,* **12,** 276 (1979).
19. W. Burchard, M. Schmidt, and W. H. Stockmayer, *Macromolecules,* **13,** 1265 (1980).
20. B. Chu, I. H. Park, Q. W. Wang, and C. Wu, *Macromolecules,* **20,** 2833 (1987).
21. B. Chu and C. Wu, *Macromolecules,* **21,** 1729 (1988).

Received January 23, 1995
Revised April 20, 1995
Accepted May 9, 1995